HIGH-ASPECT-RATIO THREE-DIMENSIONAL POLYMER AND METALLIC MICROSTRUCTURES USING TWO-PHOTON POLYMERIZATION

A Thesis

by

ETHAN LAO VARGAS

Submitted to the Graduate and Professional School of
Texas A&M University
in partial fulfillment of the requirements for the degree of

MASTER OF SCIENCE

Chair of Committee,	Arum Han
Committee Members,	Hangue Park
	Jun Zou
	Victor Ugaz
Head of Department,	Aniruddha Datta

May 2022

Major Subject: Electrical Engineering

ABSTRACT

Achieving small feature microelectromechanical system (MEMS) fabrications is currently very challenging when the 3D microstructure is not feasibly compatible with conventional 2D lithography workflow. Here in this thesis, we present a fabrication process using two-photon-lithography (2PP) printing with electroless plating as an alternate method of fabricating conductive 3D MEMS structures. In the process of this, the effect of 2PP processing parameters on SU-8 photoresist is explored. These parameters include laser power, pre-baking and post-baking temperature, and slicing and hatching distance. Aspect ratio limits were also tested, reaching a consistent aspect ratio of 12 for pillars and trenches. The fabricated MEMS device is evaluated in terms of observed accuracy and reproducibility. With the results of this research, the limitations caused by current MEMS fabrication processes will be surpassed, allowing a variety of new MEMS designs to be created.

DEDICATION

To my family and significant other for supporting me, and to Dr. Arum Han and fellow lab group member, Can Huang, for helping and mentoring me throughout.

ACKNOWLEDGEMENTS

I would like to thank Dr. Arum Han for his help and guidance as my advisor and committee chair. I would also like to give thanks to Dr. Hangue Park, Dr. Jun Zou, and Dr. Victor Ugaz for lending their time to be a part of my committee and help with my academic endeavors.

I would also like to give thanks to my fellow lab group members, especially Jose Wippold for his help in the research area and Can Huang for mentoring and assisting me throughout my research work.

Finally, I would like to thank my graduate program assistant and the other department staff for helping guide me throughout my time at Texas A&M University.

CONTRIBUTORS AND FUNDING SOURCES

Contributors

This work was supervised by a thesis committee consisting of Professor Arum Han (Chair), Dr. Hangue Park, and Dr. Jun Zou of the Department of Electrical Engineering and Dr. Victor Ugaz of the Department of Chemical Engineering.

All the work for this thesis was completed by the student under the advisement and mentorship of Dr. Arum Han of the Department of Electrical Engineering and Can Huang of Nanobio Systems Lab. The electroless plating optimization and work was done by Zhiyu Yan from Dr. Jun Zou's lab.

Funding Sources

Graduate study was supported by the Ebensberger fellowship and scholarships from the Texas A&M University Department of Electrical and Computer Engineering. This work was also supported by an assistantship sponsored by Harold White (Limitless Space, Houston, TX). The contents of this work are solely the responsibility of the student and do not necessarily represent the official views of Limitless Space.

NOMENCLATURE

MEMS	Microelectromechanical Systems
CMOS	Complementary Metal-Oxide-Semiconductor
2D	Two Dimensional
3D	Three Dimensional
2PP	Two-Photon Polymerization
DI	Deionized
NA	Numerical Aperture
PGMEA	Propylene Glycol Methyl Ether Acetate
IPA	Isopropyl Alcohol
EDS	Energy-Dispersive Spectroscopy

TABLE OF CONTENTS

LIST OF FIGURES

LIST OF TABLES

1. INTRODUCTION

Microelectromechanical systems (MEMS) are a part of many everyday devices, such as printers, phones, and cars. Accelerometers, gyroscopes, microphones, and many other kinds of sensors make up MEMS devices. To fabricate MEMS, several common photolithography methods are used: bulk micromachining, surface micromachining, deep reactive-ion etched silicon micromachining, CMOS MEMS, and microstructural molding process. Bulk micromachining involves removing material from the substrate that the MEMS device is being built on, which is often a silicon wafer. This is done in certain patterns or depths to create certain features needed in the MEMS device. Surface micromachining involves adding material onto the substrate surface and taking away the added material in certain locations, creating additional layers of features for MEMS. Deep reactive-ion etched silicon micromachining involves the use of deep reactive-ion etching, which is the main method for fabricating high-aspect-ratio features in MEMS. CMOS MEMS involves the use of CMOS foundry processes to create MEMS. Lastly, microstructural molding process involves creating molds on a substrate with a photosensitive polymer (like SU-8) and pouring a silicone resin onto the mold to cure and pull off to create the MEMS structures. Complexity and cost of the MEMS devices increases with the addition of layers from these processes, with each microstructure layer design limited to the mask in a 2D plane [1].

Two-photon polymerization (2PP) is a recent method of micron scale 3D printing that can create complex polymer structures [2]. 2PP uses a laser to selectively cure certain voxels of a resin printing material to create 3D structures. This enables easy fabrication of complex multi-layer MEMS structures with a single 3D 2PP print. 2PP also allows for the fabrication of 3D structures such as inclines and hills to be printed, which are difficult or impossible to realize with

standard MEMS fabrication processes. Although 2PP has these capabilities, 2PP printing is only limited to polymer materials, which are typically not highly conductive. Conductive structures are useful in many MEMS sensors due to the interaction of MEMS devices with electrical components to operate and give sensor data. [3] With access to only polymer materials, it limits the use of 2PP to fabricate only certain MEMS devices. As a result, recent research has been done exploring the use of 2PP to print conductive structures.

One example of conductive structures being printed with 2PP is in reference [4]. It was done by first 2PP printing structures with a photoresist/ICP precursor formulation, then doing oxidative polymerization of the ICP precursor to make the polymer conductive, with conductivity of 0.04 S/cm. Another example of 2PP printed conductive structures is in reference [5]. Here, they mixed metal particles with a polymer resin, then 2PP printed structures with this mixture. After 2PP, the structures were pyrolyzed, getting rid of the polymer material and leaving the metal particles behind in the shape of the 2PP printed structures but shrunken in size. Another method of printing conductive structures with 2PP is using electroless plating to selectively coat a polymer in metal. In reference [6], this is done using 2PP to fabricate 3D SU-8 structures, then using electroless plating to selectively coat the SU-8 in silver. Out of the current methods of fabricating conductive structures with 2PP, the electroless plating method used in reference [6] was chosen to be used due to its good conductivity (compared to reference [4]) and structure accuracy (compared to reference [5]) in its results.

Electroless plating is the use of a chemical bath to coat a material in metal.[3] It differs from electroplating by not needing an externally generated electric current. As a method of metallization, electroless plating has the advantages of being able to selectively coat a material and coat a structure on all sides [6]. This differs from common MEMS metallization/metal

deposition methods, which can be directional, nonselective, and/or incompatible with polymers [6]. For the silver electroless plating method, it involves plasma treatment and Tollens' reagent to selectively coat the commonly used polymer, SU-8, in silver [6]. This method was chosen over other electroless plating methods [7] due to silver's high conductivity. SU-8 has also been used before in 2PP printing [8-16], allowing this method to be possible. With the use of 2PP and silver electroless plating, the fabrication of high aspect ratio metallized 3D polymer structures is presented in the following thesis.

2. PRELIMINARY EXPERIMENTS

To determine a target structure to be fabricated with 2PP, a couple initial experiments were done with a high-resolution proprietary resin (IP-Dip, Nanoscribe) for the 2PP machine used (Photonic Professional GT, Nanoscribe). The 2PP machine's highest resolution objective (63x 1.4 NA) was used with the substrate in the dip-in laser lithography configuration and IP-Dip 63x Fused Silica (3D SF) recipe [17], which is the default recipe for the IP-Dip resin with the 63x objective on this 2PP machine. After 2PP, the sample was developed for 2 minutes in PGMEA, then rinsed in isopropyl alcohol for 5 minutes (see procedure in appendix A.1).

For the first initial prints, cylindrical pillars were printed with a height of 30 µm and diameters ranging from 1.5 µm to 4 µm in increments of 0.5 µm. This was done in order to test the aspect ratio limits of the IP-Dip resin. Each pillar was printed 27 times, and they were observed with a 10x lens on a standard microscope. From what was observed, 2 out of 27 pillars collapsed with diameter of 4 µm, 2 out of 27 pillars collapsed with a diameter of 3.5 µm, 0 out of 27 pillars collapsed with a diameter of 3 µm, 0 out of 27 pillars collapsed with a diameter of 2.5 µm, 19 out of 27 pillars collapsed with a diameter of 2 µm, and 27 out of 27 pillars collapsed

with a diameter of 1.5 µm. From this, it appeared that 30 µm tall pillars with a diameter of 2.5 µm can consistently be printed with the IP-Dip resin. When testing this pillar diameter value between circular and square pillars, square pillars were found to be better at not collapsing. This was tested with a linear array set of 3 pillars spaced 10 µm apart. With a height of 30 µm and a diameter or side length of 2.5 µm, 0 out of 8 sets of square pillars collapsed while 8 out of 8 sets of circular pillars collapsed. This is summarized in table 1 below.

Varying Pillar Diameter	Pillar Diameter (µm)	1.5	2	2.5	3	3.5	4
	Number of Pillars Collapsed (out of 27)	27	19	0	0	2	2
Cylindrical vs. Square Pillars	Pillar Type	Cylindrical			Square		
	Number of Pillars Collapsed (out of 8)	8			0		

Table 1: Results of initial pillar tests with IP-Dip resin

From these results, a target structure was designed to test the capabilities of 2PP printing. The target structure can be seen below in figure 1. The goal of this structure was to test the high aspect ratio capabilities of 2PP with SU-8 by printing out pillars and a trench between walls. The design also displays the unique capabilities of 2PP printing with inclines and curved surfaces.

Another goal of this structure was to test the feasibility of an electrostatic actuation MEMS device, which is done by putting a potential difference across one side wall structure and the middle pillars structure. Two types of wall structures were designed: the triangular supported wall and an arch supported wall, which can be seen in figure 1 below. The dimensions in red (pillar thickness and distance between the pillar and wall) were pursued to be as small as possible without structure collapse.

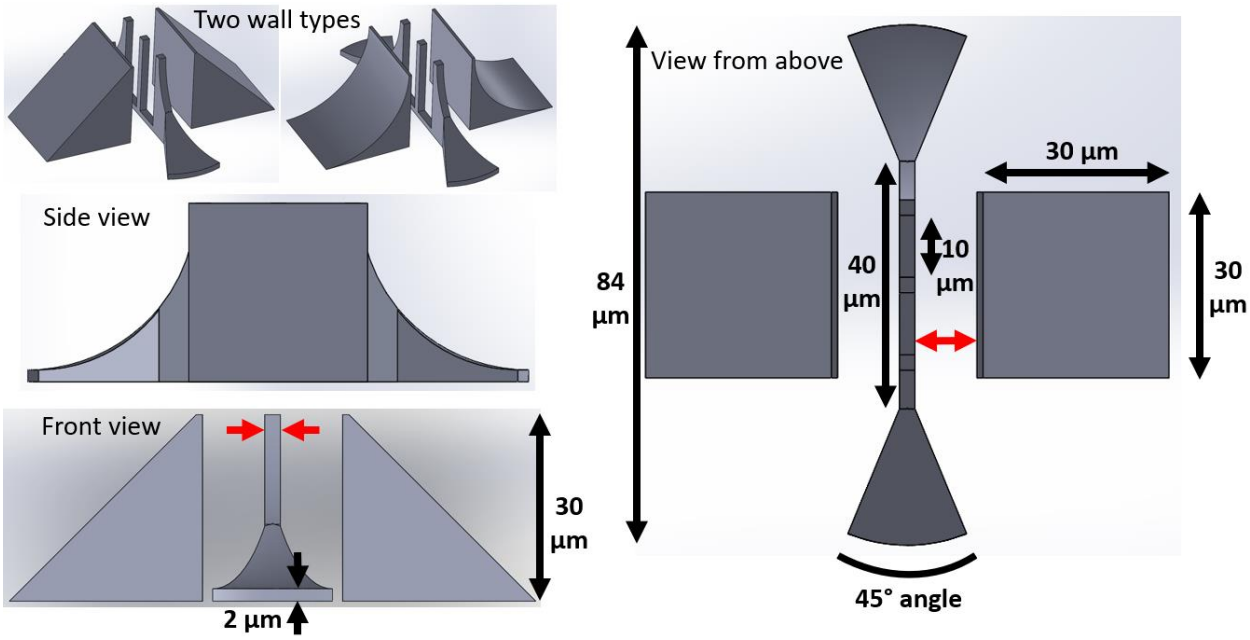

Figure 1: Target structure for 2PP printing

This new design was used to test a different rinsing chemical, Novec 7500, and compare it to IPA. This was tested with a pillar thickness of 2.5 µm, triangular and arch supported wall designs, and pillar to wall distances of 1, 2.5, 5, 7.5, 10, 12.5, and 15 µm. Results were observed with a 5x and 20x lens on a standard microscope. With IPA, 13 out of 14 of the structures had partially collapsed, while only 4 out of 14 of the pillar arrays collapsed with Novec 7500. This

information is shown in more detail in table 2 below. From this experiment, Novec 7500 appeared to show better results than IPA. The pillar dimensions of square 2.5 µm side length pillars and process step of using Novec 7500 for rinsing after development were kept and used as starting point variables for the 2PP tests with SU-8.

Did the structure collapse?								
Pillar to Wall Distance (µm)		1	2.5	5	7.5	10	12.5	15
IPA Rinsing Chemical	Triangular Support Design	Yes	Yes	Yes	Yes	Yes	No	Yes
	Arch Support Design	Yes	Yes	Yes	Yes	Yes	Yes	Yes
Novec 7500 Rinsing Chemical	Triangular Support Design	Yes	Yes	No	No	No	No	No
	Arch Support Design	Yes	Yes	No	No	No	No	No

Table 2: Detailed summary of results comparing rinsing chemicals IPA and Novec 7500

3. MATERIALS / METHODS

2.1 Proposed Fabrication Workflow

To create 3D polymer metallic microstructures, three processes were implemented in this work: metal patterning to interface with the 3D structures, two-photon polymerization (2PP) to create the 3D polymer structures, and electroless plating to selectively metalize the 3D

structures. Process optimization was first done for the two-photon polymerization and the electroless plating processes to achieve high aspect ratio structures and uniform metal coating. Optimization and the materials and methods used for each of these processes are described in the following sections.

2.3. Two-Photon Polymerization with SU-8

Using the results from the preliminary experiments, a procedure and structure design for 2PP with SU-8 was developed. For the general procedure of doing 2PP using SU-8, approximately 40 µm of SU-8 2025 was first spin coated on a bare 2 inch silicon wafer (100 rpm/s to 500 rpm for 5 s, then 300 rpm/s to 2000 rpm for 30 s, then 5 s deceleration to 0 rpm). The sample was then soft baked at 65 then 95 °C for 5 and 15 minutes respectively. After waiting for the sample to return to room temperature, 2PP printing was done. Once 2PP printing was complete, the sample was post exposure baked at 65 then 95 °C for 1 and 6 minutes respectively. After waiting for the sample to return to room temperature, it was developed in propylene glycol monoethyl ether acetate (PGMEA, Millipore Sigma, MA) for approximately 10 minutes, followed by a rinse in Novec 7500 for approximately 15 s, another development of an additional 2 minutes in a new PGMEA bath, another rinse for approximately 15 s in Novec 7500, and finally drying the sample for approximately 10 s on a hot plate set to 100 °C. This general process is shown in figure 2 below (see procedure in appendix A.2).

For the initial 2PP process parameters, the 2PP machine's online manual and guide, NanoGuide,[17] was used to determine initial values for testing. These values were the following: laser scan speed of 10000 µm/s, laser power of 15 mW, slicing and hatching distance of 0.25 µm, and the rest of the parameters being from the IP-Dip 63x Fused Silica (3D SF) recipe. To

find the optimal process parameters, the soft and post bake temperatures were varied (baking temperatures of 85, 90, 95, and 100 °C were tested in place of the main temperature, 95 °C, stated in the general procedure), the slicing and hatching distance was varied (slice/hatch distances of 0.2/0.2, 0.25/0.25, 0.3/0.3, 0.4/0.4, and 0.3/0.2 µm were tested), and the exposure dosage from the laser power was varied (laser powers of 10, 15, and 20 mW were tested). The slicing and hatching distance values were chosen based on NanoGuide's recommendation for SU-8 printing of a slicing and hatching distance between 0.25 and 0.5 µm and having slicing distance equivalent to hatching distance. The slicing and hatching distance of 0.3 and 0.2 µm is the default parameters used for printing with the IP-Dip resin. The laser power values were chosen to be around NanoGuide's recommended value of 15 mW for printing with SU-8.

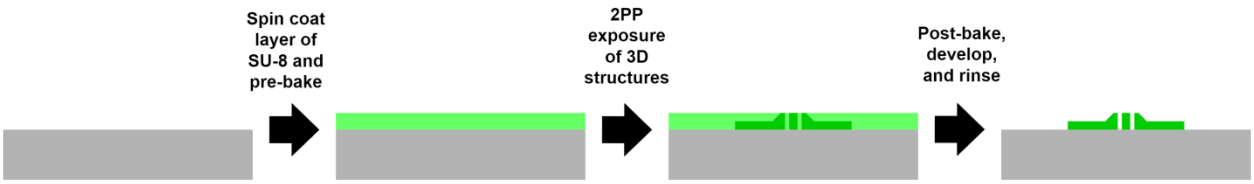

Figure 2: General process for 2PP with SU-8

2.4. Electroless Plating

Electroless plating was done after the 2PP printed SU-8 structures have been realized. The general process for the electroless plating was the following: use O_2 plasma at a low power level to treat the TPP SU-8 samples for 5 minutes under 350 mTorr and room temperature, prepare Tollens reagent with varying concentrations of $AgNO_3$ (0.85 to 4.25 g/L), immerse the sample in 20 ml of Tollens reagent at temperatures varying from 24 to 35 °C, add 1 ml of varying concentrations of glucose (0.33 to 2 g/L) and wait for 3 minutes for a single

electroplating cycle, and repeat the last step for a varying amount of cycles (3 to 7). After the electroplating, the sample is taken out of the liquid and dried. To prepare the Tollens reagent, 10 wt.% Ammonium Hydroxide was added dropwise into $AgNO_3$ solution until the precipitate disappears.

2.4. Metal Patterning

Once 2PP printing with SU-8 and electroless plating was optimized, metal patterning was explored to interface with the electroplated SU-8 structures. The metal patterned electrodes are printed onto the substrate before the 2PP process. One method the metal patterning was done was by using an additive transfer process, which was the following: spin coat (100 rpm/s for 5 s to 500 rpm for 5 s, then 300 rpm/s for 5 s to 3000 rpm for 45 s) a silicon wafer with AZ5214 positive photoresist, soft bake the sample at 105 °C for 5 minutes, wait for the sample to return to room temperature, expose the pattern in a mask aligner for 100 mJ/cm^2, develop the sample in AZ726, rinse the sample in DI water and blow dry, deposit metal with an electron beam evaporator (PVD 75, Kurt J. Lesker Company), strip the rest of the photoresist in AZ400T, and rinse with DI water and blow dry (see procedure in appendix A.3).

Another method the metal patterning was done was by using the subtractive transfer process, which was the following: deposit metal with an electron beam evaporator, spin coat (100 rpm/s for 5 s to 500 rpm for 5 s, then 700 rpm/s for 5 s to 4000 rpm for 40 s) a silicon wafer with AZ5214 positive photoresist, bake the sample at 105 °C for 1 minute, wait for the sample to return to room temperature, expose the mask pattern in a mask aligner for 85 mJ/cm^2, bake the sample at 120 °C for 2 minutes, expose the sample without the mask pattern in a mask aligner for 200 mJ/cm^2, develop the sample in AZ726 until exposed photoresist is removed, rinse with DI water and blow dry, etch the sample in a chromium etch bath only until chromium electrode

pattern is complete, rinse with DI water and blow dry, strip the sample in AZ400T, and rinse the sample once more with DI water and blow dry (see procedure in appendix A.4).

2.5. Characterizations

To analyze the 2PP printed results, the sample was first either sputter coated with gold or electroless plated. The sample was then imaged with a scanning electron microscope (MIRA3 FE-SEM, TESCAN). Structures were observed for accuracy to desired design and if the structure had collapsed or not. To determine the quality of the electroless plating, energy-dispersive spectroscopy (EDS) analysis was used to determine the material contents of the sample, which was done using a focused-ion beam instrument (Helios NanoLab 460F1, FEI).

3. RESULTS

3.1. 2PP Printing and Parameter Optimization

With the results from these 2PP tests with IP-Dip and the recommended printing parameters for SU-8 from Nanoguide, SU-8 structures were printed with varying parameters to see the effect the parameter has on the structure and to improve the 2PP accuracy with SU-8 as much as possible. To test the effect of baking temperature on the 2PP results, 2.5, 2, and 1.5 µm cubes were printed, and the vertical and horizontal side lengths of the results were measured from the top view. These measurements were taken with the measurement tool in the SEM machine. To determine accuracy of the results, percent error was calculated with the sum of all the vertical and horizontal side lengths for a certain baking temperature and laser power. For these prints, the slicing and hatching distance were set to 0.25 µm, the scan speed was kept at 10000 um/s, and the laser power was set to 15 mW. Other than the varied baking temperatures,

the rest of the general procedure was kept the same. These prints and measurements were then repeated with a laser power of 17.5 mW. These results are summed up in table 3 below. As a result of this data, 95 °C was kept as the baking temperature for any following 2PP prints.

Laser Power	15 mW				17.5 mW			
Baking temperature (°C)	85	90	95	100	85	90	95	100
2.5 µm cube vertical side length	2.45	2.45	2.4	2.49	2.61	2.73	2.61	2.55
2.5 µm cube horizontal side length	2.78	2.82	2.76	2.83	3.02	3.05	2.98	2.95
2 µm cube vertical side length	1.95	1.97	2.26	2	2.07	2.23	2.1	2.03
2 µm cube horizontal side length	2.26	2.32	1.94	2.34	2.46	2.59	2.41	2.45
1.5 µm cube vertical side length	1.41588	1.40689	1.35243	1.42218	1.44403	1.55227	1.45184	1.54827
1.5 µm cube horizontal side length	1.70004	1.74853	1.6585	1.75794	1.78434	1.73595	1.73846	1.87795
Percent Error (%)	**4.63267**	**5.96183**	**3.09108**	**7.001**	**11.5698**	**15.7352**	**10.7525**	**11.7185**

Table 3: Measurement results from varying baking temperature

For the variation of slicing and hatching distance parameters in 2PP printing, the target structure was printed with a wall to pillar distance of 7.5 µm and a pillar thickness of 2.5 µm. The images below (figure 3) compares the resulting 2PP prints of varying slicing and hatching distances. Scan speed was kept at the default 10000 µm/s, and laser power was set to the NanoGuide recommended 15 mW. The general procedure stated in the materials and methods sections was followed for the rest of the variables. As a result of these images, a slicing and hatching distance of 0.25 µm was kept for any following 2PP prints.

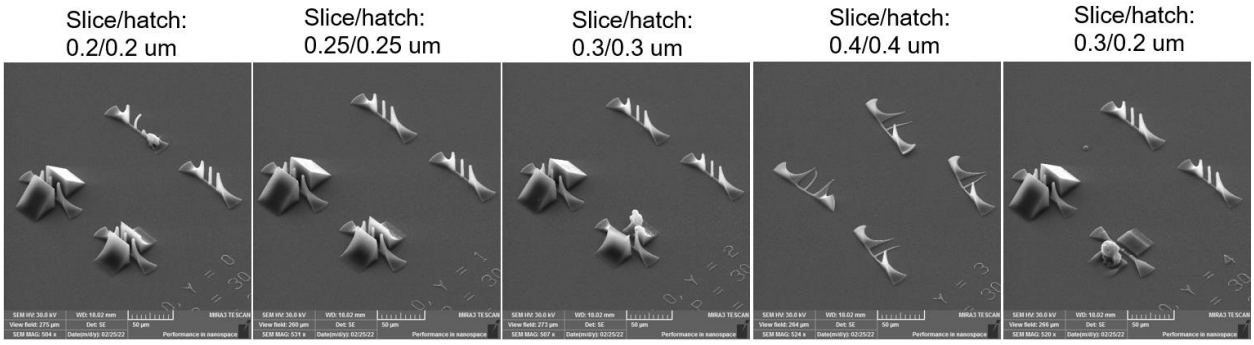

Figure 3**:** SEM images of the SU-8 structures with varying slicing and hatching distances

The effect of varying 2PP exposure dosages can be seen in the image below (**Figure 5**). For these prints, the slicing and hatching distance were again set to 0.25 µm, the scanning speed was set to 10000 µm/s, and the baking temperature was set close to 95 °C. Other than the varied laser power to vary exposure dosages, the general procedure was kept the same. The designs printed here are similar to the previous designs as well, with wall to pillar distance being approximately 15 µm.

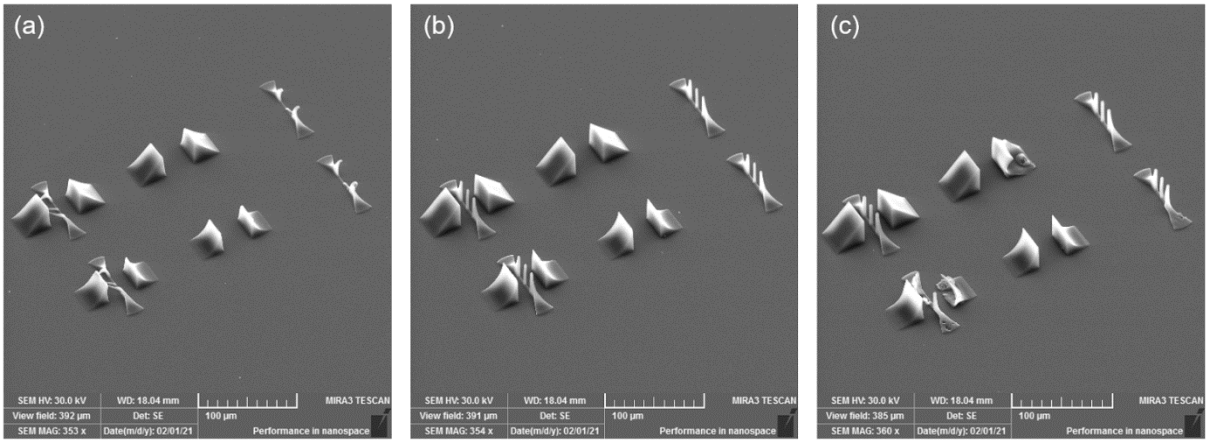

Figure 4: SEM images of the SU-8 structures with exposure laser powers of (a) 10 mW, (b) 15 mW, and (c) 20 mW

3.2. Electroless Plating and Validation

For the optimization of electroless plating, several parameters were considered, being glucose concentration (varied from 0.33 to 2 g/L), $AgNO_3$ concentration (varied from 0.85 to 4.25 g/L), plating temperature (varied from 24 to 35 °C), and number of plating cycles (varied from 3 to 7). Tests showed that a lower plating temperature and more cycles resulted in a smoother coating, and for both chemicals, thinner solutions resulted in better quality coatings. As a result, the optimized electroless plating parameters were a glucose concentration of 0.33 g/L, a $AgNO_3$ concentration of 4.25 g/L, a plating temperature of 24 °C, and a number of cycles of 5. These values were chosen based on good smoothness of coating, good selectivity of coating, and low process time.

Validation that the SU-8 structures were successfully electroplated by Ag (resistivity of around 1.9e-6 to 7.6e-6 [Ω-m]) can be seen in the right images below using EDS (figure 5). In figure 5, the left image shows the selectivity of the electroless plating despite excessive deposition. The right images show that silver has successfully been plated along the entire wall

through EDS analysis. The design of these structures are again the target design, with their wall to pillar gap being approximately 2.5 µm.

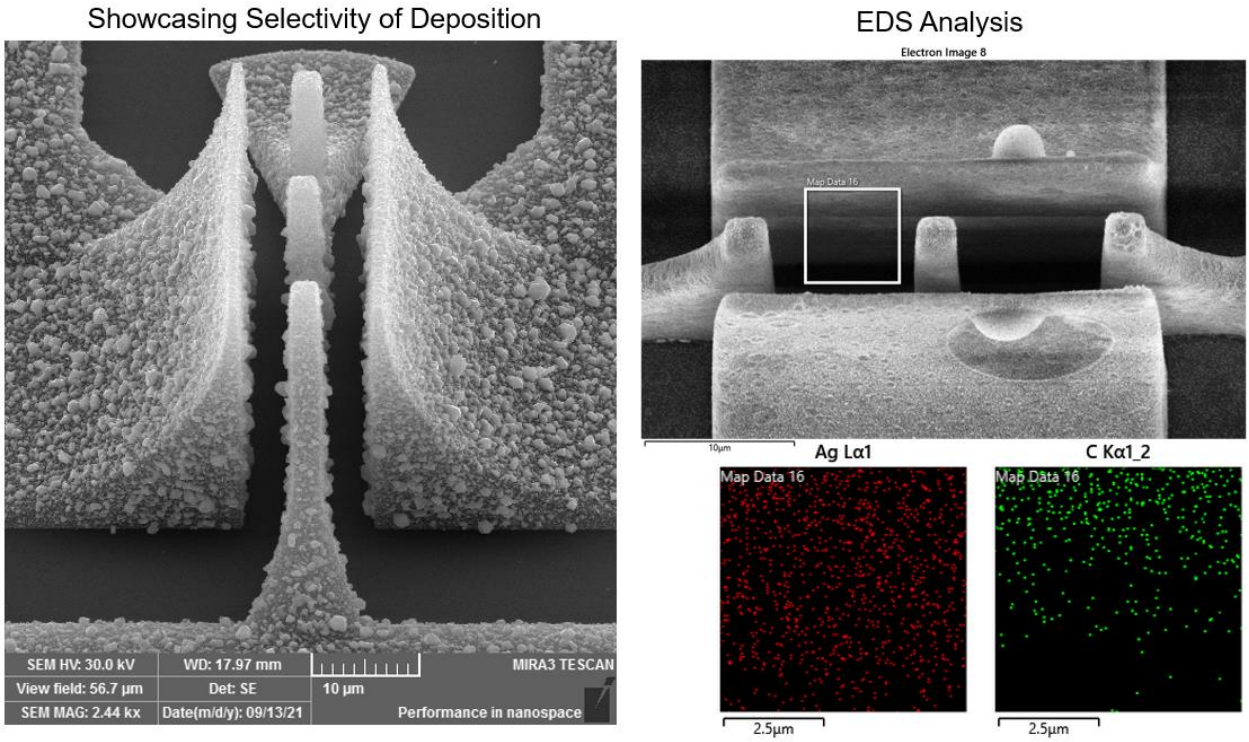

Figure 5: SEM image and EDS analysis of an electroplated SU-8 structure

3.3. Metal Patterning Electrodes with 2PP

For the fabrication of metal patterning electrodes to interface with the SU-8 structures, copper was experimented with as a metal patterning material due to its high cocnductivity. The results of creating copper electrodes and the effect on the electrodes after electroless plating can be seen below in figure 6 (mask used in appendix C.1). This was done with the additive transfer process, with the copper thickness being 100 nm and deposition done in an electron beam

evaporator at 0.2 nm/s. The copper electrodes were connected with 660 µm long, 50 µm wide, and 10 µm thick block of SU-8.

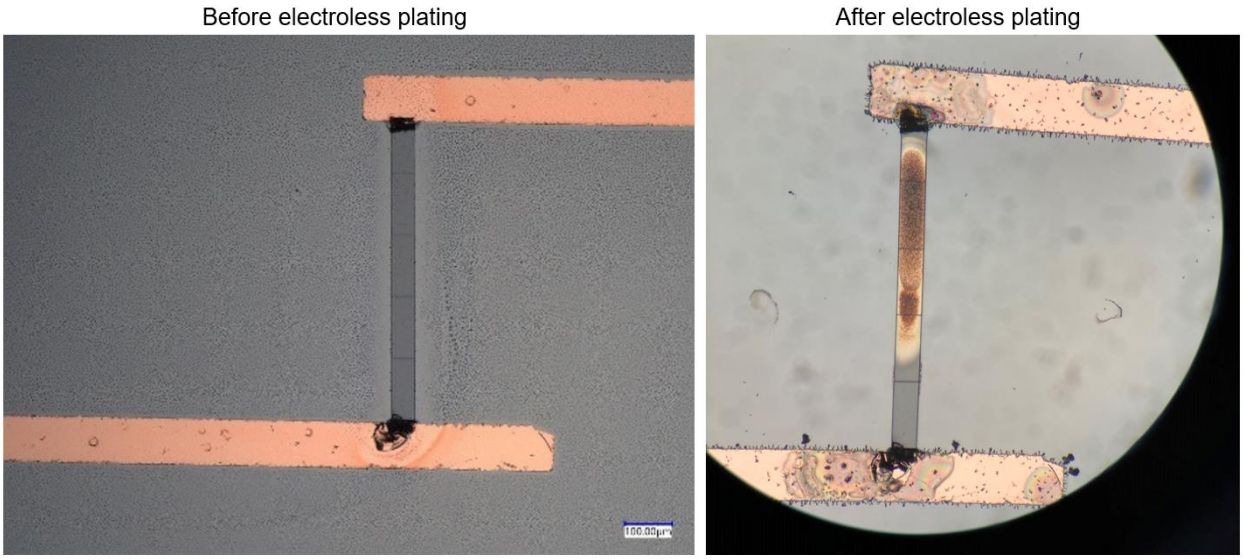

Figure 6: Images before and after electroless plating of Cu electrodes

From the metal patterning results in figure 6, copper did not seem to work well with SU-8. From here, chromium electrodes were tested with the subtractive transfer process. The results before and after electroless plating of Cr electrodes can be seen in figure 7 below. This was done with 150 nm thick of Cr deposited at 0.18 nm/s in an electron beam evaporator. To describe figure 7 below, the lighter colored area in the image before electroless plating is the chromium patterned area (mask used in appendix C.2). The distance between the black arrows in the before and after electroless plating images is the same distance in the metal pattern design. The gap distance values stated in the images after electroless plating are the distances between the top

pair and bottom pair of chromium traces. The red orange shade in the images after electroless plating is silver from the electroless plating.

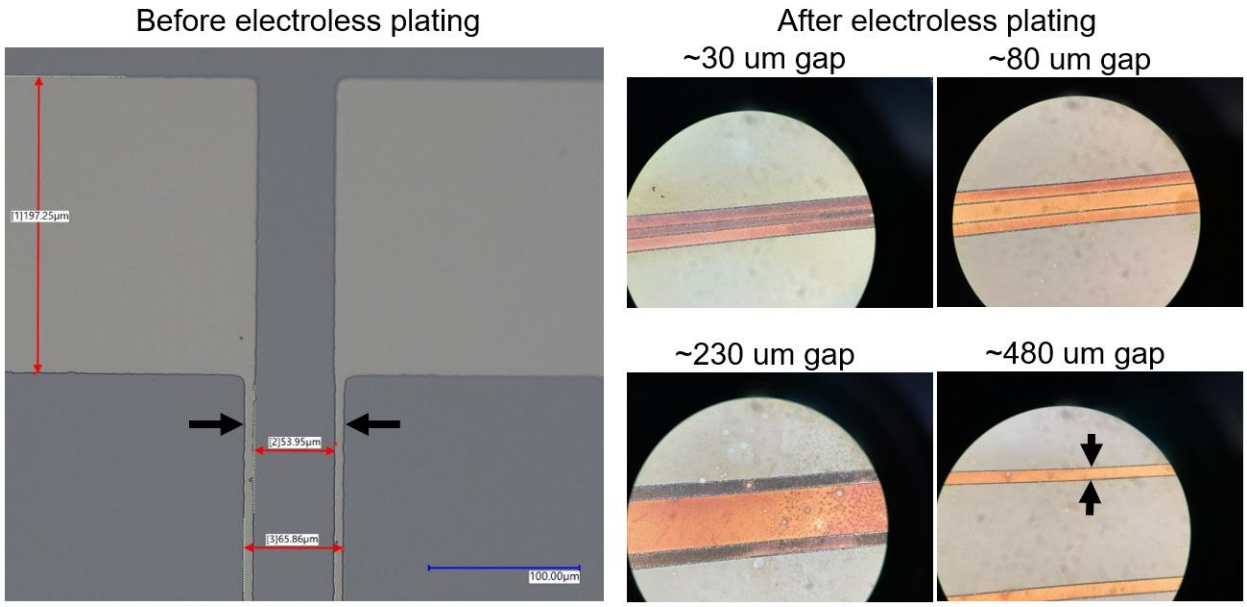

Figure 7: Images before and after electroplating of Cr electrodes

From the results in figure 7, the silver deposition appeared to short the area between chromium traces. In an attempt to counter this, an SiO2 layer was deposited under the chromium layer to try to prevent this silver deposition as well as reduce the electrical signal loss across the bare silicon substrate. The results for this after electroless plating are shown in figure 8 below. In figure 8, the left two images show a modified target design for electrostatic actuation tests, with SU-8 branching out from a wall and pillar support being shrunken on one side of the structure (see appendix B.5 for 3D model dimensions). Fabrication of this structure was done similarly as structures before, the only difference being a reduced laser power of SU-8 structures printed over the Cr traces (see structures and laser powers in figure 11). This is done to prevent the resin from

bubbling due to increased laser reflection near the substrate surface during 2PP printing. The purple area of the left and right image is the SiO2 surface, while the bluish area in the left image is silver. The Cr electrodes and traces in figure 8 were created using the mask in appendix C.3.

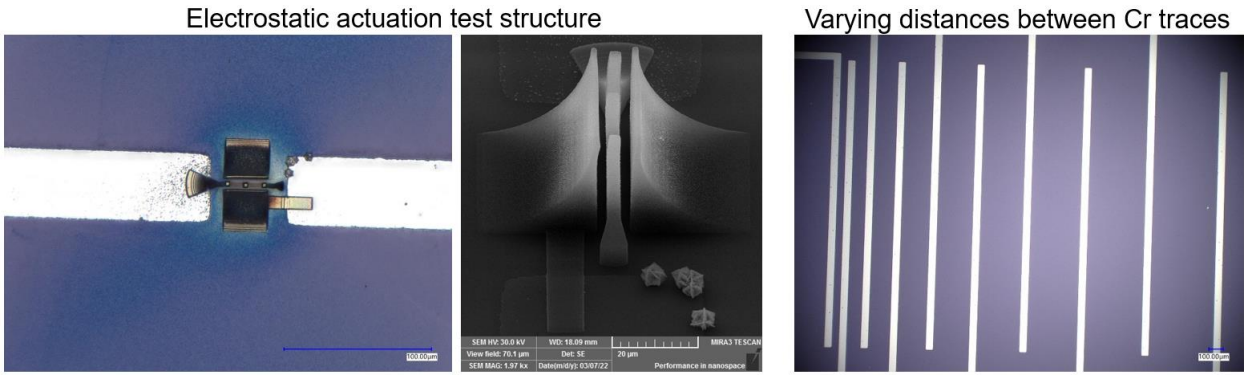

Figure 8: Images after electroless plating of metal pattern on SiO2

4. DISCUSSION

4.1 Parameter Variance with 2PP and Electroless Plating

From the results shown in table 3, it seems that more testing is needed to determine the effect of baking temperature on 2PP printing with SU-8. From this data, it appears that a baking temperature of 95 °C has the highest accuracy for both laser powers, but there is no obvious trend with a decrease or increase in baking temperature. To further prove this, in figure 9 below, the target structure with a pillar to wall distance of ~2.5 µm was printed at each of the varied baking temperatures at a laser power of 15 mW. From these results, it can be seen that despite the change in baking temperature, structure accuracy appears to be kept, with the slight exception of the structures resulted at a baking temperature of 100 °C shown in figure 9 below, where the

pillars between walls are shown to have collapsed against the side wall. To conclude, baking temperatures around 85 to 95 °C work well with 2PP printing with SU-8, but as your baking temperature increases more than that, there is a chance of weaker polymerized structures.

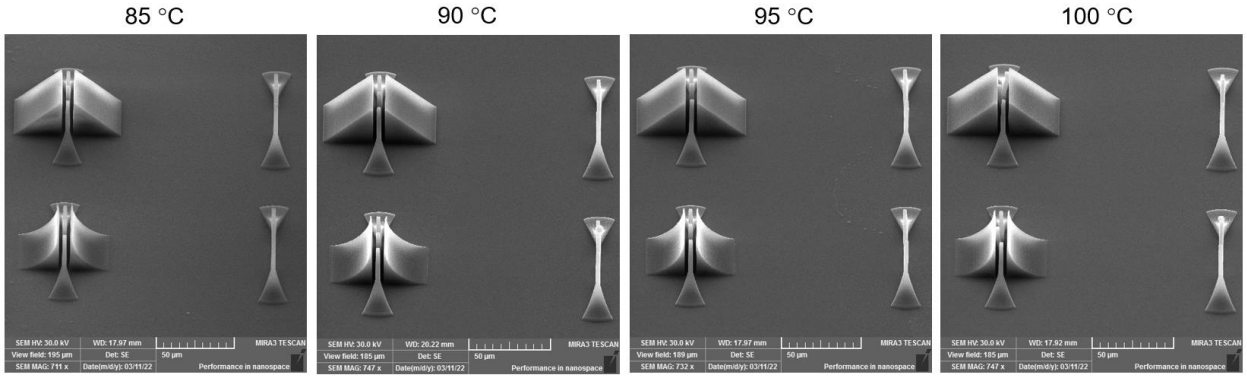

Figure 9: Target structure printed at varied baking temperatures

From the results shown in figure 3, slicing and hatching distance have a some effect on the accuracy of the printed 2PP SU-8 structures. With too small a slicing or hatching distance, the possibility of overexposure increases, which can be seen in the deformed structures caused by bubbling in the rightmost and leftmost images of figure 3. It can also be seen that with too high of a slicing and hatching distance, the polymer structures are weaker, causing collapse, which can be seen in the image of structures printed with a slicing and hatching distance of 0.4 µm. This is most likely due to insufficient polymerization of the SU-8 resin.

The results in figure 4 show how increasing 2PP exposure (by increasing laser power) can help with SU-8 structure strength and polymerization of the SU-8, but with too much exposure, some bubbling can occur, causing structure deformities, as seen in figure 4(c) on the bottom structure. As a result, with the set scan speed of 10000 µm/s, laser power should not deviate far from 15 mW or there will be a risk in causing the SU-8 to bubble and structures to

deform. Table 3 also shows that an increase in laser power slightly increases the size of the structure, with 22 out of 24 of the measurements showing an increase in cube size when the laser power was adjusted from 15 mW to 17.5 mW.

With the results from the varied baking temperatures, slicing and hatching distances, and laser powers, a baking temperature of 95 °C, a slicing and hatching distance of 0.25 µm, and a laser power of 15 mW was chosen as the optimal parameters for the fabrication of the target structure. With these parameters, the structure shown in figure 10 below can be consistently and successfully printed without any structure collapse. In this structure, a wall to pillar gap of <2.5 µm was achieved with pillars approximately 2.5 µm thick, all at a height of about 30 µm. This means that an aspect ratio of ~12 was achieved. The 3D model dimensions of this structure can be seen in the appendix (appendix B.1 to B.4).

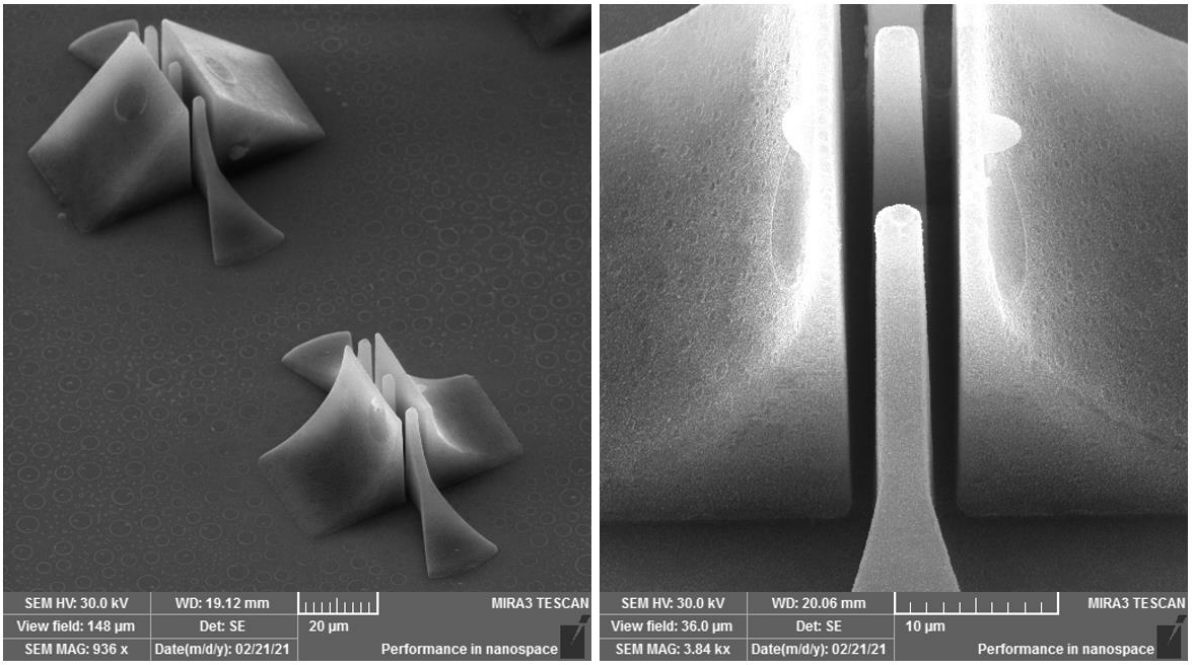

Figure 10: Electroless plated target structure printed with optimized parameters

In a few further electroless plating tests, the effect of electroless plating was tested on a SU-8 structures with varied exposure dosages. The results can be seen below in figure 11. It can be seen that a laser power increase from 10 mW to 11 mW resulted in clumpier deposition of silver. As laser power was increased further, deformities caused by overexposure of the resin started to be seen with little or no difference to the quality of the silver coating of the structures.

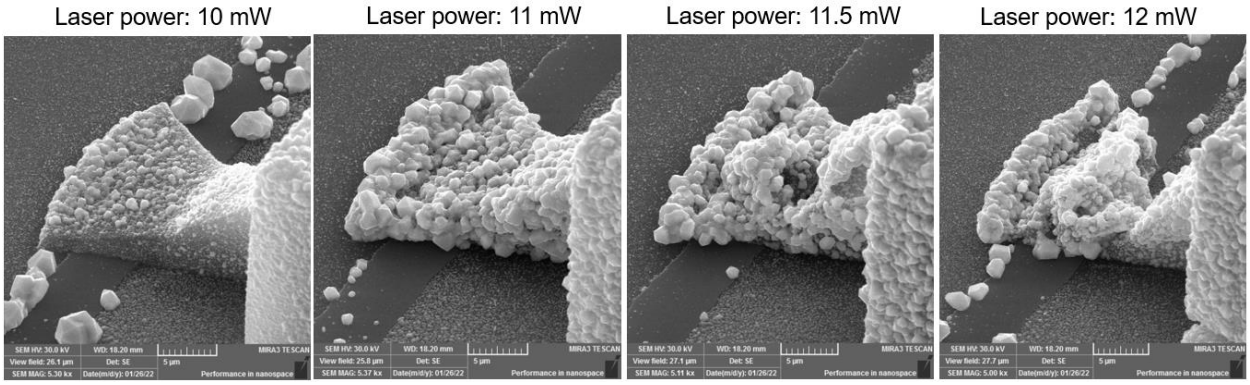

Figure 11: Effect of laser power on electroless plating

4.2 Metal Patterned Electrodes

From the results shown in figure 6, it can be seen that the copper electrodes reacted with the electroless plating solution, preventing silver deposition at the SU-8 and copper interface. As a result, chromium electrodes were attempted, as can be seen in figure 7. With chromium electrodes, another issue appeared with silver being deposited between nearby adjacent traces, shorting the chromium pattern. This deposition appeared to stop at a trace to trace distance between 230 and 480 µm. As a result, adding an SiO2 layer was attempted before depositing chromium to see if the less conductive surface would help prevent unwanted silver deposition. These results are shown in figure 8, and it can be seen that while adding the SiO2 layer stopping the unwanted silver deposition between nearby adjacent chromium traces (right image of figure

8), it also brought bad deposition selectivity for the SU-8 structures. This is seen in the right image of figure 8, where silver can be seen deposited all around the target SU-8 structure, shorting the electrode pattern and the SU-8 structure. From these results, it appears that if chromium is wanting to be used as the metal patterning material, bare silicon would work with a specially designed metal pattern that reduces the area that a chromium trace is near another chromium trace to a minimum. This would come at the expense of more electrical signal loss across the bare silicon substrate.

4.3 Future Work and Summary

With the results collected in this thesis, there are several areas of future work that can be done. Process parameter variance can be expanded to find a more definite range of values that can consistently produce accurate results. Some additional parameters can also be looked at, such as the contouring feature in 3D design processing, other rinsing chemicals, and laser scan speed. In terms of the electrode metal pattern, chromium with a specialized electrode design to prevent unwanted silver deposition could be used to interface with the structures fabricated, but it has yet to be tested. Other metals can also be explored, such as gold, which is known as an inert metal and most likely would not react with the electroless plating solution. From these electrode tests, a sample MEMS device could be fabricated and tested as a proof of concept of this MEMS fabrication method. While a sample device as been designed and fabricated, it has yet to be tested for its accuracy and function. Another area that future work can be done in is analysis of the electroless plating quality. For example, determining the thickness or roughness of the silver coating was not done.

A collection of all the results on 2PP printing SU-8 of the target structure can be seen in the table below (table 4). To summarize, there is a certain range of soft and post bake temperatures, slicing/hatching distance parameters, and 2PP exposure dosage parameters that are needed to achieve accurate high aspect ratio 2PP printed SU-8 structures. These ranges are approximately shown in the table below, but further testing is needed to validate the exact error amount allowed in these parameters. For example, all of the structures printed that resulted in bubbling below had successfully printed at least part of the 3D target design. This could mean that the bubbling that had happened was a rare occurrence, caused possibly by an air bubble in the resin or some other slight variation in fabrication.

Laser Power (mW)	Scan Speed (µm/s)	Slicing Distance (µm)	Hatching Distance (µm)	Baking Temperature (C)	Bubbling?	Structure Collapse / Quality?
15	10000	0.25	0.25	85	No	Accurate
15	10000	0.25	0.25	90	No	Accurate
15	10000	0.25	0.25	100	No	Slight collapse
15	10000	0.2	0.2	95	Yes	Deformed
15	10000	0.3	0.3	95	Yes	Deformed
15	10000	0.4	0.4	95	No	Collapse, structure partially formed
15	10000	0.3	0.2	95	Yes	Deformed
10	10000	0.25	0.25	95	No	Structure partially formed
20	10000	0.25	0.25	95	Yes	Deformed
15	10000	0.25	0.25	95	No	Accurate

Table 4: Summary of the parameters tested for 2PP printing the target structure with SU-8

5. CONCLUSION

High-aspect ratio metallized 3D structures have been realized with the procedure and parameters developed in this thesis. In addition to this, some initial results have been shown on interfacing the structures with electrodes. Nonetheless, the results from this thesis have shown that the use of 2PP and electroless plating of SU-8 can be used to surpass current limitations in current MEMS fabrication methods in terms of 3D structure complexity. With this research, it can lead to many new MEMS devices or improvements on current MEMS designs, utilizing new 3D features such as inclines and hills to achieve improved performance in sensing and function.

REFERENCES

[1] Lawes, R. A. (2007). Manufacturing costs for microsystems/MEMS using high aspect ratio microfabrication techniques. *Microsystem technologies*, 13(1), 85-95.

[2] Lee, K. S., Yang, D. Y., Park, S. H., & Kim, R. H. (2006). Recent developments in the use of two-photon polymerization in precise 2D and 3D microfabrications. *Polymers for advanced technologies*, *17*(2), 72-82.

[3] Spearing, S. M. (2000). Materials issues in microelectromechanical systems (MEMS). *Acta materialia*, 48(1), 179-196.

[4] Kurselis, K., Kiyan, R., Bagratashvili, V. N., Popov, V. K., & Chichkov, B. N. (2013). 3D fabrication of all-polymer conductive microstructures by two photon polymerization. *Optics express*, *21*(25), 31029-31035.

[5] Vyatskikh, A., Delalande, S., Kudo, A., Zhang, X., Portela, C. M., & Greer, J. R. (2018). Additive manufacturing of 3D nano-architected metals. *Nature communications*, *9*(1), 1-8.

[6] Yan, Y., Rashad, M. I., Teo, E. J., Tanoto, H., Teng, J., & Bettiol, A. A. (2011). Selective electroless silver plating of three dimensional SU-8 microstructures on silicon for metamaterials applications. *Optical Materials Express*, *1*(8), 1548-1554.

[7] Dai, W., & Wang, W. (2007). Selective metallization of cured SU-8 microstructures using electroless plating method. *Sensors and Actuators A: Physical*, *135*(1), 300-307.

[8] Wu, D., Chen, Q. D., Niu, L. G., Wang, J. N., Wang, J., Wang, R., ... & Sun, H. B. (2009). Femtosecond laser rapid prototyping of nanoshells and suspending components towards microfluidic devices. *Lab on a Chip*, 9(16), 2391-2394.

[9] Williams, H. E., Diaz, C., Padilla, G., Hernandez, F. E., & Kuebler, S. M. (2017). Order of multiphoton excitation of sulfonium photo-acid generators used in photoresists based on SU-8. *Journal of Applied Physics*, *121*(22), 223104.

[10] Shao, Y., Zhao, Y. A., Ma, H., Li, C., Li, D., & Shao, J. (2019, July). Efficient method for determination of laser conditions adopted in laser-induced micro-lithology based on laser polymerization size analysis. In *Tenth International Conference on Thin Film Physics and Applications (TFPA 2019)* (Vol. 11064, p. 110640R). International Society for Optics and Photonics.

[11] Kumi, G., Yanez, C. O., Belfield, K. D., & Fourkas, J. T. (2010). High-speed multiphoton absorption polymerization: fabrication of microfluidic channels with arbitrary cross-sections and high aspect ratios. *Lab on a Chip*, *10*(8), 1057-1060.

[12] Seet, K. K., Juodkazis, S., Jarutis, V., & Misawa, H. (2006). Feature-size reduction of photopolymerized structures by femtosecond optical curing of SU-8. *Applied physics letters*, *89*(2), 024106.

[13] Amato, L., Keller, S. S., Heiskanen, A., Dimaki, M., Emnéus, J., Boisen, A., & Tenje, M. (2012). Fabrication of high-aspect ratio SU-8 micropillar arrays. *Microelectronic engineering*, *98*, 483-487.

[14] Ohlinger, K., Lin, Y., Poole, Z., & Chen, K. P. (2011). Undistorted 3D microstructures in SU8 formed through two-photon polymerization. *AIP Advances*, *1*(3), 032163.

[15] Lin, Y., Gao, C., Gritsenko, D., Zhou, R., & Xu, J. (2018). Soft lithography based on photolithography and two-photon polymerization. *Microfluidics and Nanofluidics*, *22*(9), 1-11.

[16] Hu, Q., Liu, Y., He, Y., Zhang, F., Wildman, R., Tuck, C., & Hague, R. (2015). Fabrication of 3D polymer-metal nano-composites in a single step by two photon induced polymerisation and metal salt reduction. In *Int. Solid Freeform Fabrication Symposium* (pp. 1036-1042).

[17] Nanoscribe. (2016). *NanoGuide*. https://support.nanoscribe.com/hc/en-gb

APPENDIX A

FABRICATION PROCEDURES

A.1: Two-Photon Polymerization Fabrication Procedure for IP-Dip

1. Place a drop of IP-Dip on a clean substrate
2. Insert substrate with the 63x objective into 2PP machine in the dip-in laser lithography configuration
3. Find substrate interface and determine location of print wanted on the 2PP machine
4. 3D print the desired design with laser exposure in the IP-Dip resin on the 2PP machine
5. Once printing is complete, develop the sample upside down in PGMEA for 2 minutes
6. Rinse the sample upside down in the rinsing chemical (IPA or Novec 7500) for 5 minutes
7. Set the sample right side up and let it air dry

A.2: Two-Photon Polymerization Fabrication Procedure for SU-8

1. Place approximately 2 ml of SU-8 2025 in the center of a 2 inch silicon wafer
2. Spin coat the SU-8 on the wafer for an approximate thickness of 40 μm with the following steps:
    a. Accelerate at 100 rpm/s for 5 s to 500 rpm
    b. Stay at 500 rpm for 5 s
    c. Accelerate at 300 rpm/s for 5 s to 2000 rpm
    d. Stay at 2000 rpm for 30 s
    e. Decelerate at 400 rpm/s to 0 rpm
3. Soft bake the sample on a hot plate with the following steps:

    a. Place the sample on a hot plate at 65 °C for 5 minutes
    b. Immediately transfer sample to a hot plate at 95 °C (or the varied baking temperature) for 15 minutes
4. Remove sample from hot plate and wait until the sample is at room temperature
5. Place a drop of immersion oil onto the center of the sample
6. Insert substrate with the 63x objective into 2PP machine in the dip-in laser lithography configuration
7. Find substrate interface and determine location of print wanted on the 2PP machine
8. 3D print the desired design with laser exposure in the SU-8 resin on the 2PP machine
9. Post bake the sample on a hot plate with the following steps:
    a. Place the sample on a hot plate at 65 °C for 1 minute
    b. Immediately transfer sample to a hot plate at 95 °C (or the varied baking temperature) for 6 minutes
10. Remove sample from hot plate and wait until the sample is at room temperature
11. Develop the sample in PGMEA for 10 minutes
12. Rinse the sample in Novec 7500 for approximately 15 s
13. Develop the sample again in a new clean PGMEA bath for 2 minutes
14. Rinse the sample again in Novec 7500 for approximately 15 s
15. Set the sample on a hot plate at 100 °C for 10 s to dry

A.3: Electrode Patterning Procedure (Additive Transfer Process)

1. Place approximately 1 ml of AZ5214 Photoresist on a 2 inch silicon wafer
2. Spin coat the photoresist on the wafer with the following steps:

a. Accelerate at 100 rpm/s for 5 s to 500 rpm
b. Stay at 500 rpm for 5 s
c. Accelerate at 500 rpm/s for 5 s to 3000 rpm
d. Stay at 3000 rpm for 45 s
e. Decelerate at 600 rpm/s to 0 rpm

3. Bake the sample on a hot plate at 105 °C for 5 minutes
4. Remove sample from hot plate and wait until the sample is at room temperature
5. Expose the sample with a mask in a mask aligner for 100 mJ/cm^2
6. Develop the sample in AZ726 until the exposed photoresist is removed
7. Rinse the sample with DI water and blow dry
8. Deposit 100 nm (or desired thickness) of desired electrode material with an electron beam evaporator
9. Strip in AZ400T at 65 °C until metal electrode pattern appears
10. Rinse with DI water and blow dry

A.4: Electrode Patterning Procedure (Subtractive Transfer Process)

1. If doing an SiO2 layer, the following steps were done: (optional)
    a. Perform a buffered oxide etch clean by doing the following steps:
        i. Submerge a 2 inch silicon wafer first in acetone for 30 s
        ii. Then submerge the wafer in IPA for 30 s
        iii. Then submerge the wafer in buffered oxide etch for about 10 s
        iv. Then submerge the wafer in DI water 3 minutes
        v. Then submerge the wafer in a new clean bath of DI water for 3 minutes

vi. Blow dry the wafer once this is complete

b. Dry deposit SiO2 at 1100 °C for 30 minutes

2. Deposit 150 nm (or desired thickness) of desired electrode material with an electron beam evaporator
3. Place approximately 1 ml of AZ5214 Photoresist on a 2 inch silicon wafer
4. Spin coat the photoresist on the wafer with the following steps:
    a. Accelerate at 100 rpm/s for 5 s to 500 rpm
    b. Stay at 500 rpm for 5 s
    c. Accelerate at 700 rpm/s for 5 s to 4000 rpm
    d. Stay at 4000 rpm for 40 s
    e. Decelerate at 800 rpm/s to 0 rpm
5. Bake the sample on a hot plate at 105 °C for 1 minutes
6. Remove sample from hot plate and wait until the sample is at room temperature
7. Expose the sample with a mask in a mask aligner for 85 mJ/cm^2
8. Bake the sample on a hot plate at 120 °C for 2 minutes
9. Remove sample from hot plate and wait until the sample is at room temperature
10. Expose the sample with no mask in a mask aligner for 200 mJ/cm^2
11. Develop the sample in AZ726 until the exposed photoresist is removed
12. Rinse the sample with DI water and blow dry
13. Etch the sample in a chromium etch bath just until the metal electrode pattern appears
14. Rinse with DI water and blow dry
15. Strip in AZ400T until all the resist is off
16. Rinse with DI water and blow dry

APPENDIX B

3D MODELS PRINTED WITH 2PP (DIMENSIONS ARE IN MICRONS)

B.1: Center Pillar Structure (Nanoscribe process files: targetStructure.zip)

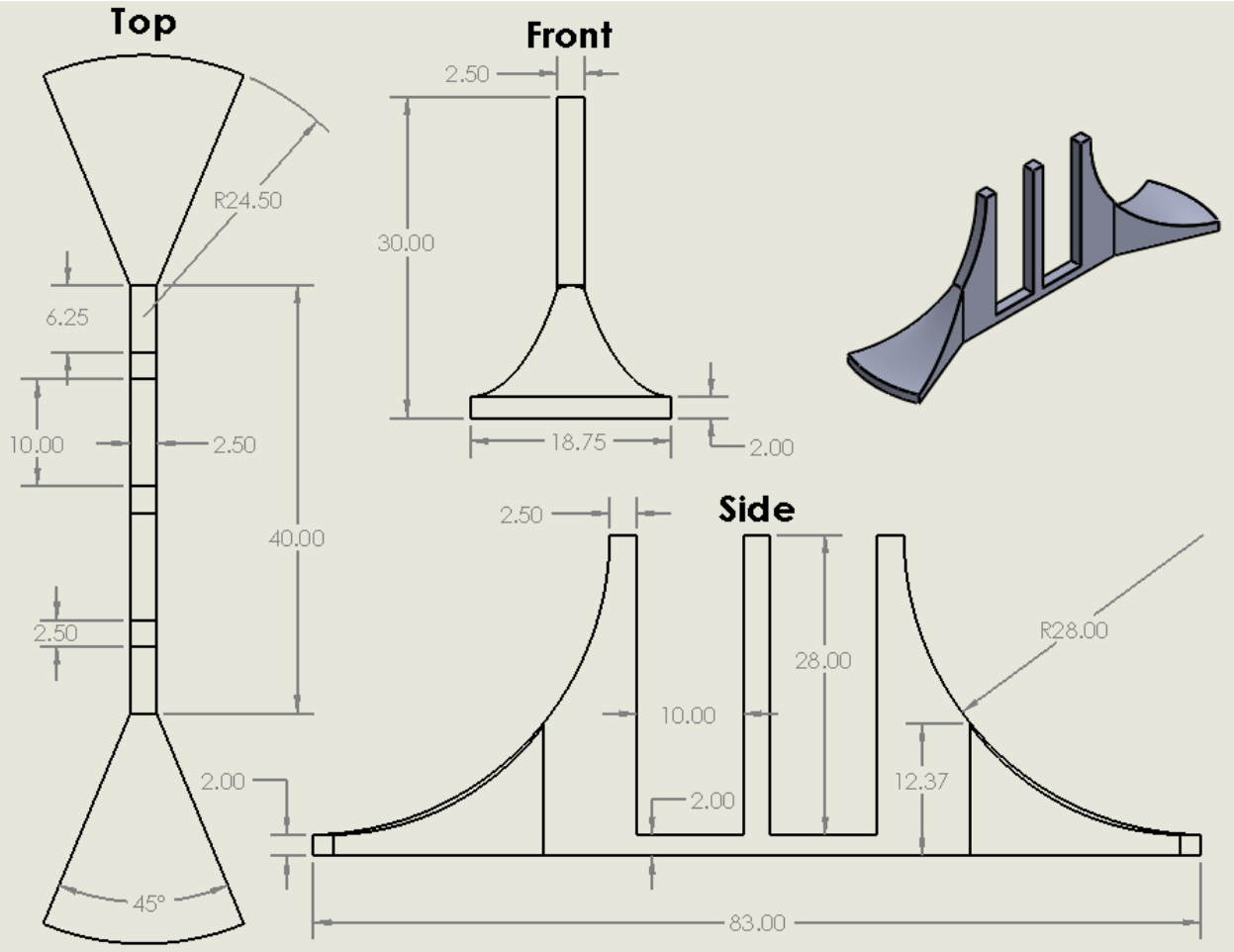

B.2: Wall Structure with Arched Support

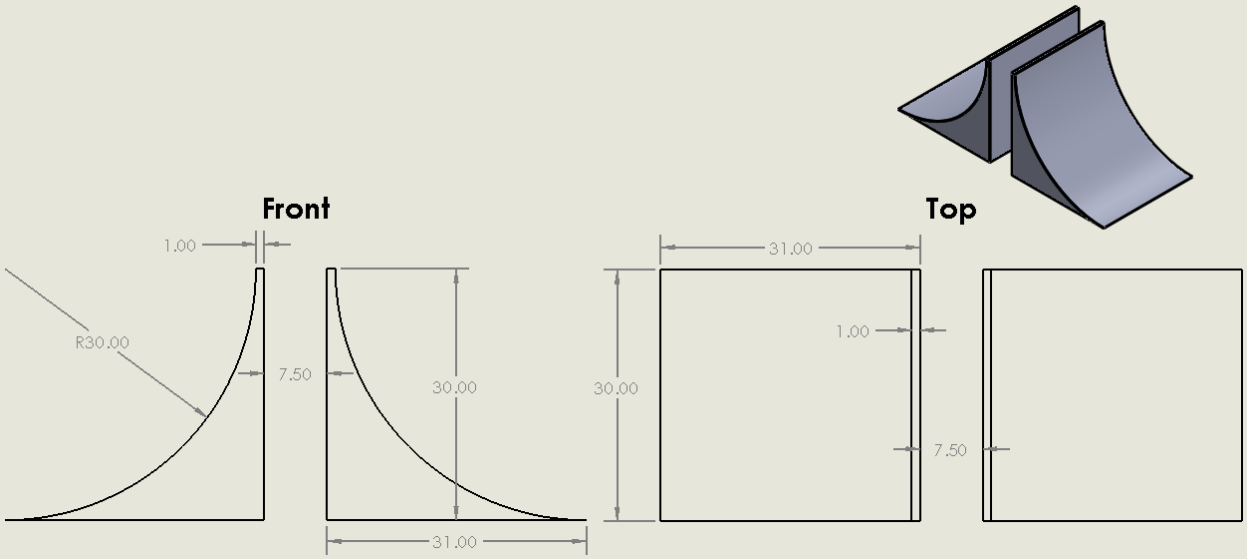

B.3: Wall Structure with Straight Support

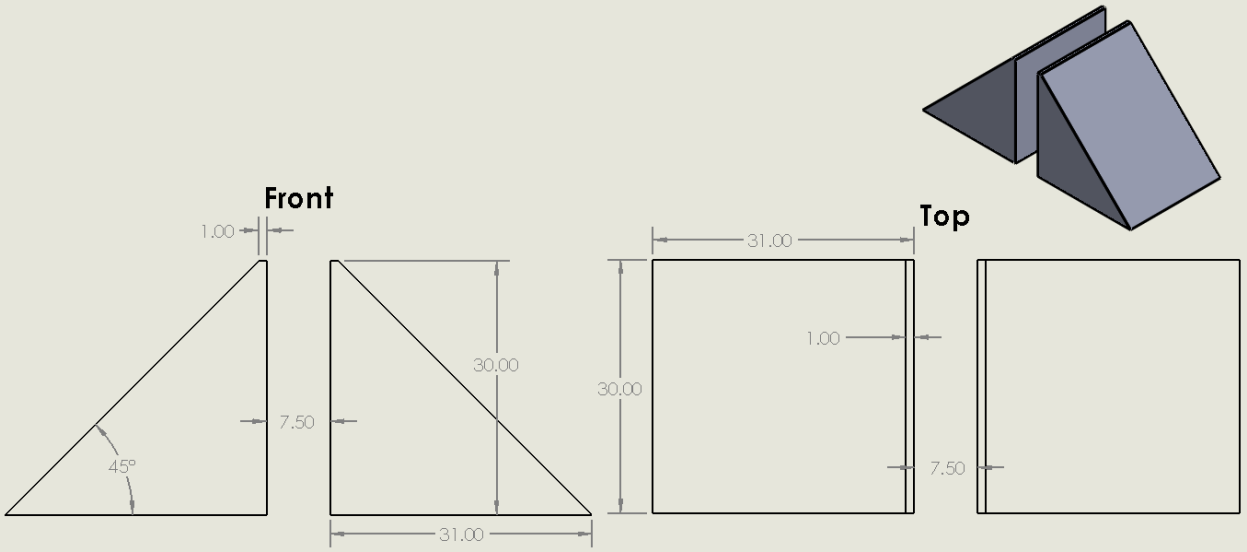

B.4: Wall and Pillar Structure (Nanoscribe process files: targetStructure.zip)

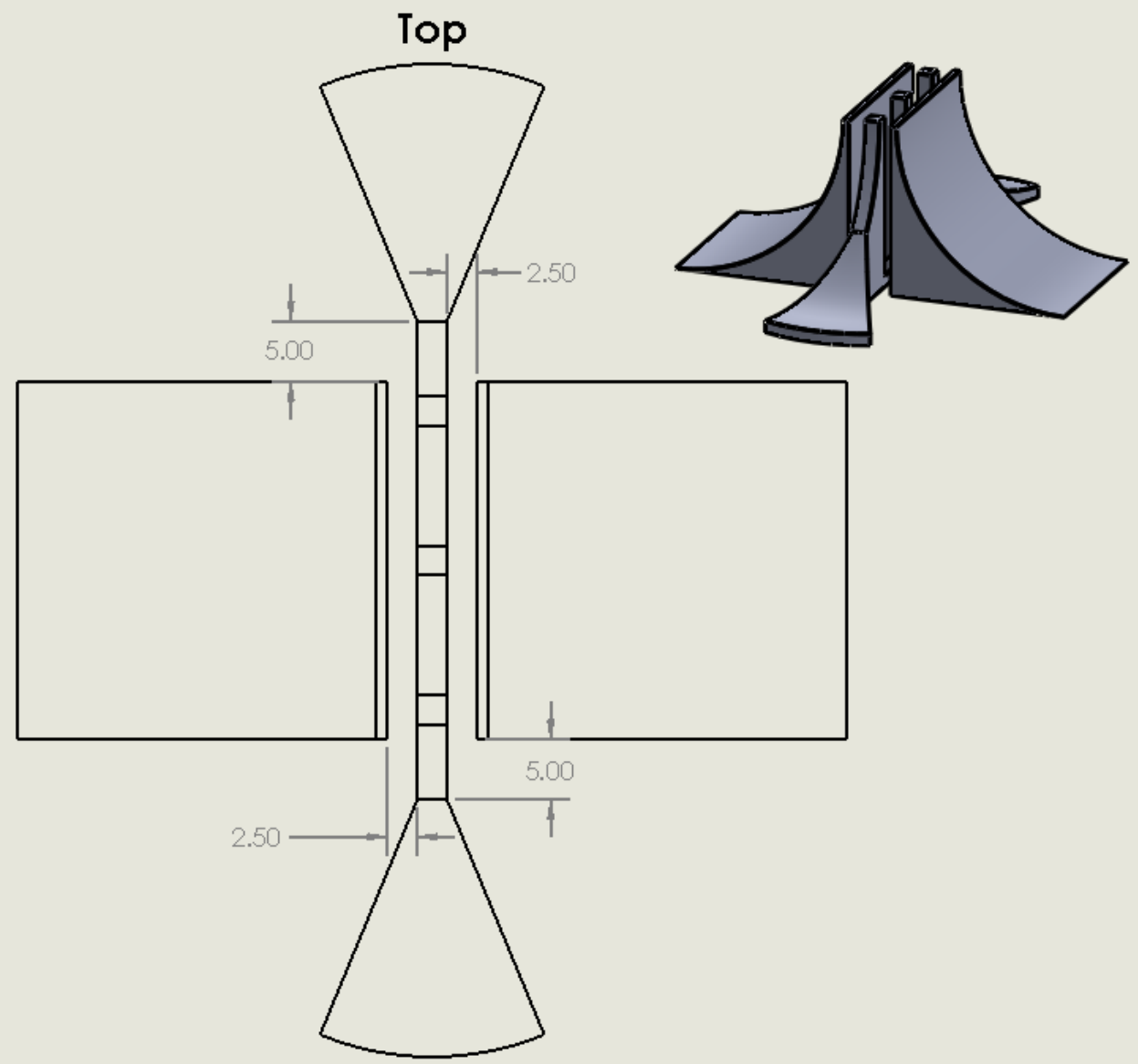

B.5: Electrostatic Actuation Structure (Nanoscribe process files: EA_Test.zip)

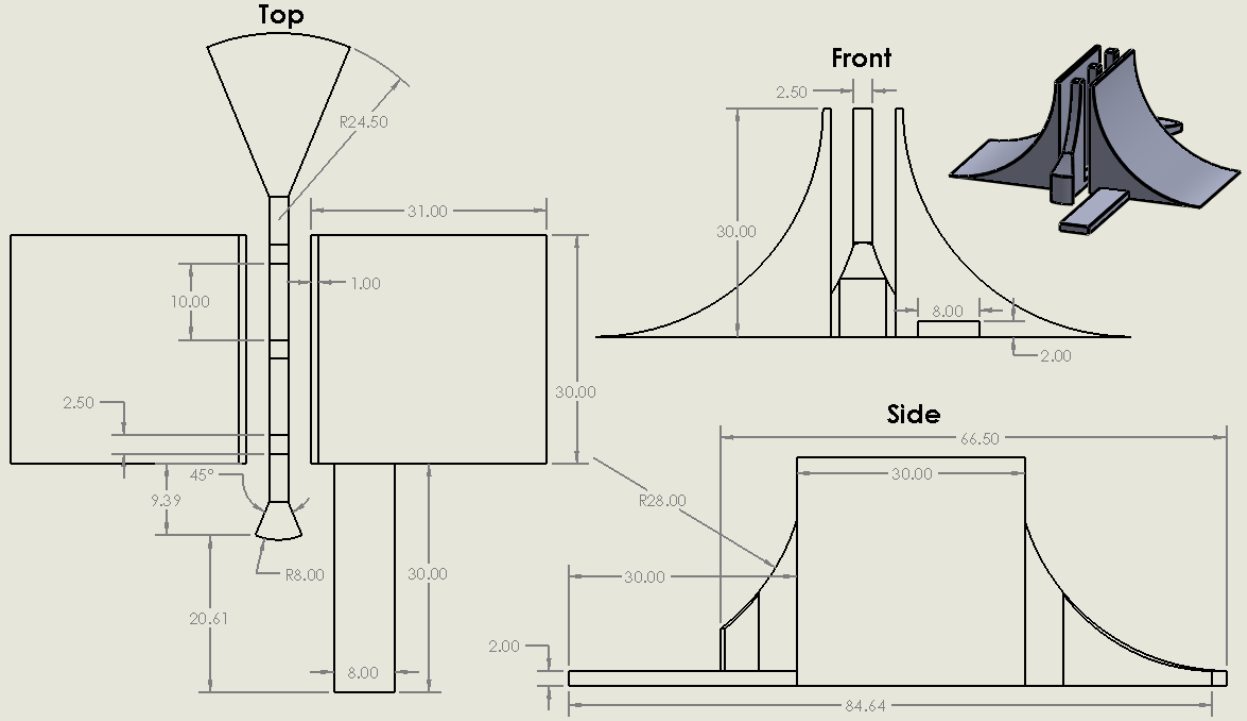

APPENDIX C

MASK DESIGNS USED FOR METAL ELECTRODE PATTERNING

C.1: Simple Electrodes Mask (file name: simpleElectrodes.dwg)

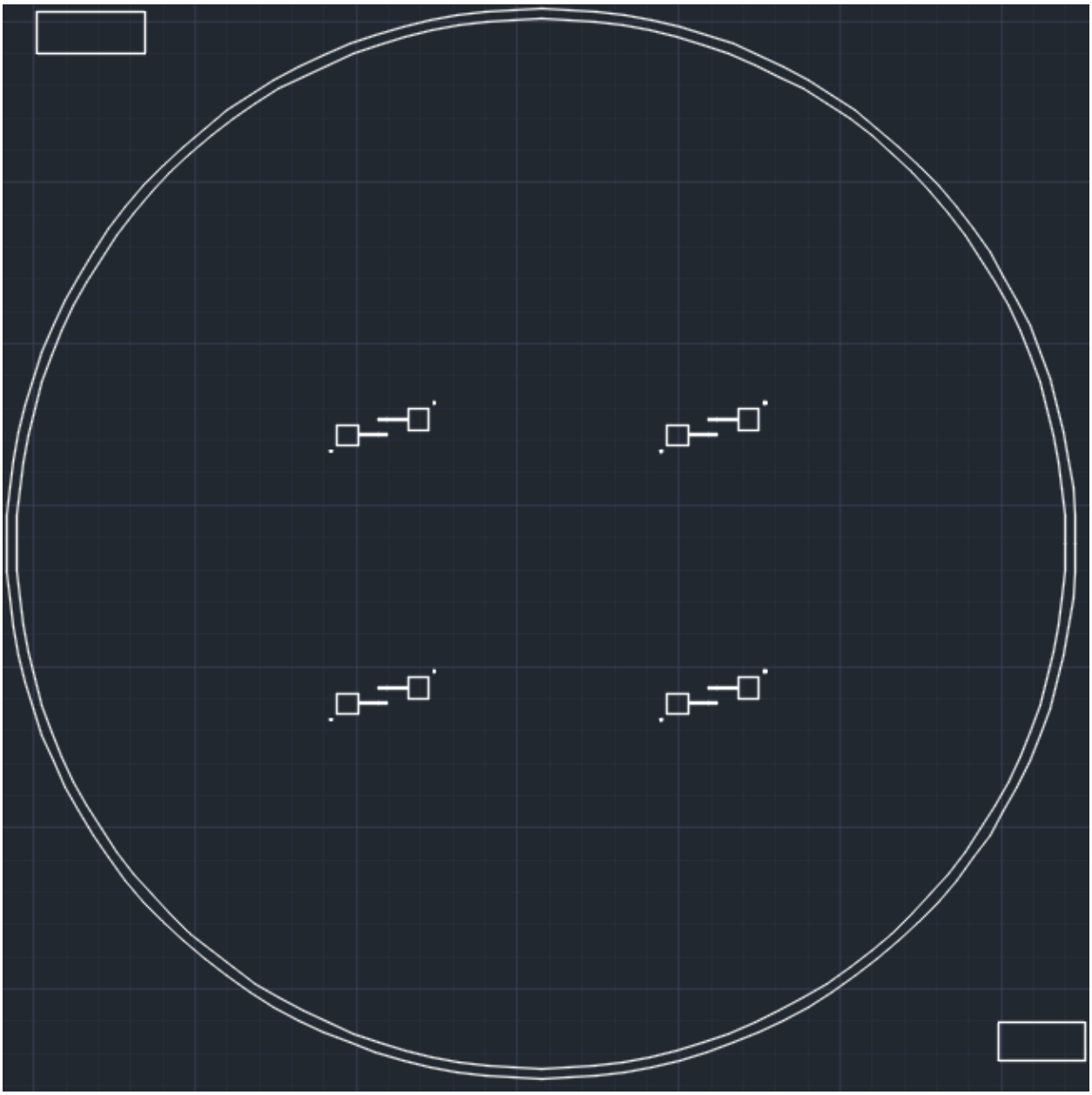

C.2: Tx/Rx Electrode Array with Varying Distances Mask (file name: TxRxArray.dwg)

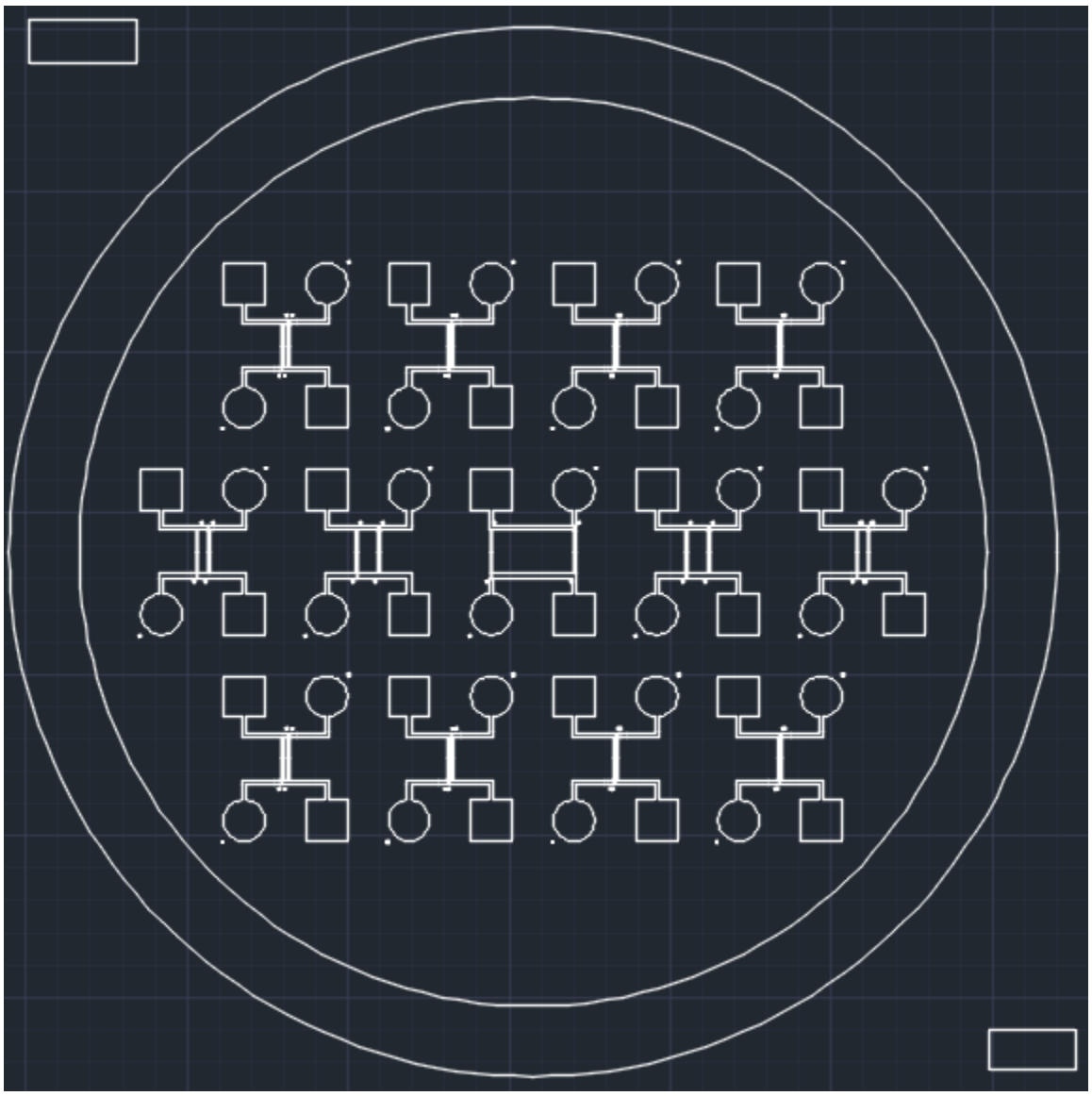

C.3: Varying Trace Distances and Single Element Mask (file name: varyingTraceDist.dwg)